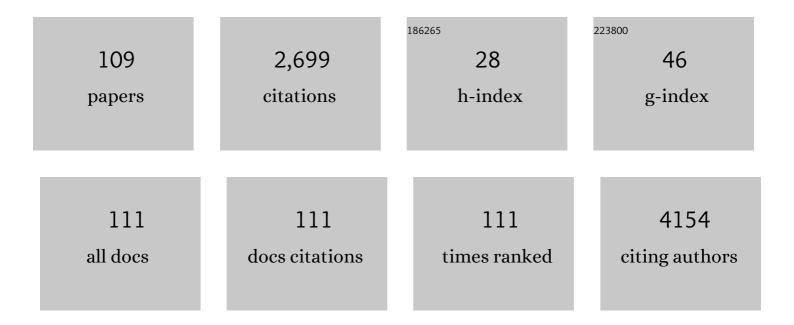
## Tsan Yao Chen

List of Publications by Year in descending order

Source: https://exaly.com/author-pdf/5473741/publications.pdf Version: 2024-02-01



#	Article	IF	CITATIONS
1	Polymorphic transition to metastable phases in hollow structured silicon anode in a Li-ions battery. Applied Materials Today, 2022, 26, 101333.	4.3	2
2	Collaboration between a Pt-dimer and neighboring Co–Pd atoms triggers efficient pathways for oxygen reduction reaction. Physical Chemistry Chemical Physics, 2021, 23, 1822-1834.	2.8	16
3	Preferential lattice expansion of polypropylene in a trilayer polypropylene/polyethylene/polypropylene microporous separator in Li-ion batteries. Scientific Reports, 2021, 11, 1929.	3.3	3
4	Tri-atomic Pt clusters induce effective pathways in a Co <sub>core</sub> –Pd <sub>shell</sub> nanocatalyst surface for a high-performance oxygen reduction reaction. Physical Chemistry Chemical Physics, 2021, 23, 18012-18025.	2.8	5
5	Interfacial atomic Ni tetragon intercalation in a NiO <sub>2</sub> -to-Pd hetero-structure triggers superior HER activity to the Pt catalyst. Journal of Materials Chemistry A, 2021, 9, 12019-12028.	10.3	19
6	Bifunctional Pt–SnO <sub>x</sub> nanorods for enhanced oxygen reduction and hydrogen evolution reactions. Sustainable Energy and Fuels, 2021, 5, 2960-2971.	4.9	10
7	NiO <sub><i>x</i></sub> -supported PtRh nanoalloy enables high-performance hydrogen evolution reaction under universal pH conditions. Sustainable Energy and Fuels, 2021, 5, 5490-5504.	4.9	14
8	Determining the Molecular Orientation on the Metal Nanoparticle Surface through Surface-Enhanced Raman Spectroscopy and Density Functional Theory Simulations. Journal of Physical Chemistry C, 2021, 125, 16289-16295.	3.1	8
9	Characterizing porous microaggregates and soil organic matter sequestered in allophanic paleosols on Holocene tephras using synchrotron-based X-ray microscopy and spectroscopy. Scientific Reports, 2021, 11, 21310.	3.3	6
10	Enhanced CO <sub>2</sub> Electrochemical Reduction Performance over Cu@AuCu Catalysts at High Noble Metal Utilization Efficiency. Nano Letters, 2021, 21, 9293-9300.	9.1	33
11	Submillisecond Laser Annealing Induced Surface and Subsurface Restructuring of Cu–Ni–Pd Trimetallic Nanocatalyst Promotes Thermal CO <sub>2</sub> Reduction. ACS Applied Energy Materials, 2021, 4, 14043-14058.	5.1	19
12	Sub-nanometer Pt cluster decoration enhances the oxygen reduction reaction performances of NiO <sub>x</sub> supported Pd nano-islands. Sustainable Energy and Fuels, 2020, 4, 809-823.	4.9	19
13	Heterogeneous NiO <sub>2</sub> -to-Pd Epitaxial Structure Performs Outstanding Oxygen Reduction Reaction Activity. Journal of Physical Chemistry C, 2020, 124, 2295-2306.	3.1	28
14	<i>In operando</i> synchrotron X-ray studies of a novel spinel (Ni <sub>0.2</sub> Co <sub>0.2</sub> Mn <sub>0.2</sub> Fe <sub>0.2</sub> Ti <sub>0.2</sub> ) <sub>3</sub> C high-entropy oxide for energy storage applications. Journal of Materials Chemistry A, 2020, 8, 21756-21770.	) <sub>4<!--<br-->10.3</sub>	sub> 66
15	An electrolyte additive with boron-nitrogen-oxygen alkyl group enabled stable cycling for high voltage LiNi0.5Mn1.5O4 cathode in lithium-ion battery. Journal of Power Sources, 2020, 477, 228473.	7.8	17
16	Recent Advancements and Future Prospects of Noble Metal-Based Heterogeneous Nanocatalysts for Oxygen Reduction and Hydrogen Evolution Reactions. Applied Sciences (Switzerland), 2020, 10, 7708.	2.5	34
17	High-Performance and Stable Hydrogen Evolution Reaction Achieved by Pt Trimer Decoration on Ultralow-Metal Loading Bimetallic PtPd Nanocatalysts. ACS Applied Energy Materials, 2020, 3, 11142-11152.	5.1	18
18	Applications of different nano-sized conductive materials in high energy density pouch type lithium ion batteries. Electrochimica Acta, 2020, 362, 137166.	5.2	4

#	Article	IF	CITATIONS
19	Keplerate-type polyoxometalate {Mo72Fe30} nanoparticle anodes for high-energy lithium-ion batteries. Journal of Materials Chemistry A, 2020, 8, 21623-21633.	10.3	20
20	<i>In Operando</i> X-ray Studies of High-Performance Lithium-Ion Storage in Keplerate-Type Polyoxometalate Anodes. ACS Applied Materials & Interfaces, 2020, 12, 40296-40309.	8.0	17
21	Promoting formic acid oxidation performance of Pd nanoparticles <i>via</i> Pt and Ru atom mediated surface engineering. RSC Advances, 2020, 10, 17302-17310.	3.6	19
22	Heterogeneous assembly of Pt-clusters on hierarchically structured CoO <sub>x</sub> @SnPd <sub>2</sub> @SnO <sub>2</sub> quaternary nanocatalysts manifesting oxygen reduction reaction performance. New Journal of Chemistry, 2020, 44, 9712-9724.	2.8	16
23	Local synergetic collaboration between Pd and local tetrahedral symmetric Ni oxide enables ultra-high-performance CO <sub>2</sub> thermal methanation. Journal of Materials Chemistry A, 2020, 8, 12744-12756.	10.3	18
24	Ir-oxide mediated surface restructure and corresponding impacts on durability of bimetallic NiOx@Pd nanocatalysts in oxygen reduction reaction. Journal of Alloys and Compounds, 2020, 844, 156160.	5.5	21
25	A highly mismatched NiO <sub>2</sub> -to-Pd hetero-structure as an efficient nanocatalyst for the hydrogen evolution reaction. Sustainable Energy and Fuels, 2020, 4, 2541-2550.	4.9	24
26	Effects of Au-Fe Nanocluster on Neuron Differentiation with Electric Stimulation. Biophysical Journal, 2020, 118, 455a.	0.5	0
27	CO-Reductive and O2-Oxidative Annealing Assisted Surface Restructure and Corresponding Formic Acid Oxidation Performance of PdPt and PdRuPt Nanocatalysts. Scientific Reports, 2020, 10, 8457.	3.3	9
28	Local Structural Disorder Enhances the Oxygen Reduction Reaction Activity of Carbon-Supported Low Pt Loading CoPt Nanocatalysts. Journal of Physical Chemistry C, 2019, 123, 19013-19021.	3.1	18
29	Conformational Effects of Pt-Shells on Nanostructures and Corresponding Oxygen Reduction Reaction Activity of Au-Cluster-Decorated NiOx@Pt Nanocatalysts. Nanomaterials, 2019, 9, 1003.	4.1	14
30	Platinum-trimer decorated cobalt-palladium core-shell nanocatalyst with promising performance for oxygen reduction reaction. Nature Communications, 2019, 10, 440.	12.8	115
31	Vanadium-based polyoxometalate as electron/ion sponge for lithium-ion storage. Journal of Power Sources, 2019, 435, 226702.	7.8	30
32	Effects of Pt metal loading on the atomic restructure and oxygen reduction reaction performance of Pt-cluster decorated Cu@Pd electrocatalysts. Sustainable Energy and Fuels, 2019, 3, 1668-1681.	4.9	19
33	Cyclability evaluation on Si based Negative Electrode in Lithium ion Battery by Graphite Phase Evolution: an operando X-ray diffraction study. Scientific Reports, 2019, 9, 1299.	3.3	5
34	H2 Reduction Annealing Induced Phase Transition and Improvements on Redox Durability of Pt Cluster-Decorated Cu@Pd Electrocatalysts in Oxygen Reduction Reaction. ACS Omega, 2019, 4, 971-982.	3.5	15
35	Influence of Glucose Derivatives on Ball-Milled Si for Negative Electrodes with High Area Capacity in Lithium-Ion Batteries. ACS Sustainable Chemistry and Engineering, 2019, 7, 2971-2979.	6.7	8
36	Atomic scale Pt decoration promises oxygen reduction properties of Co@Pd nanocatalysts in alkaline electrolytes for 310k redox cycles. Sustainable Energy and Fuels, 2018, 2, 946-957.	4.9	13

#	Article	IF	CITATIONS
37	Promotion of Ternary Pt–Sn–Ag Catalysts toward Ethanol Oxidation Reaction: Revealing Electronic and Structural Effects of Additive Metals. ACS Energy Letters, 2018, 3, 2550-2557.	17.4	41
38	Pt <sub>3</sub> clusters-decorated Co@Pd and Ni@Pd model core–shell catalyst design for the oxygen reduction reaction: a DFT study. Journal of Materials Chemistry A, 2018, 6, 23326-23335.	10.3	26
39	Mechanism of Sodium Ion Storage in Na <sub>7</sub> [H <sub>2</sub> PV <sub>14</sub> O <sub>42</sub> ] Anode for Sodiumâ€ion Batteries. Advanced Materials Interfaces, 2018, 5, 1800491.	3.7	18
40	Mechanochemical synthesis of Si/Cu3Si-based composite as negative electrode materials for lithium ion battery. Scientific Reports, 2018, 8, 12695.	3.3	8
41	Programming ORR Activity of Ni/NiO <i><sub>x</sub></i> @Pd Electrocatalysts via Controlling Depth of Surface-Decorated Atomic Pt Clusters. ACS Omega, 2018, 3, 8733-8744.	3.5	27
42	Nitrogen doping in Ta2O5 and its implication for photocatalytic H2 production. Applied Surface Science, 2018, 459, 477-482.	6.1	27
43	X-ray Absorption Spectroscopy and In-Operando Neutron Diffraction Studies on Local Structure Fading Induced Irreversibility in a 18†650 Cell with P2â€ <sup>e</sup> Na <sub>2</sub> /3Fe <sub>1</sub> /3Mn <sub>2</sub> /3O <sub>2</sub> Cathode in a Long Cycle Test. Iournal of Physical Chemistry C. 2018. 122. 12623-12632.	3.1	10
44	Crystal shape controlled H2 storage rate in nanoporous carbon composite with ultra-fine Pt nanoparticle. Scientific Reports, 2017, 7, 42438.	3.3	6
45	Enhanced electrochemical degradation of ibuprofen in aqueous solution by PtRu alloy catalyst. Chemosphere, 2017, 175, 76-84.	8.2	25
46	Heterogeneous Cu–Pd binary interface boosts stability and mass activity of atomic Pt clusters in the oxygen reduction reaction. Nanoscale, 2017, 9, 7207-7216.	5.6	21
47	The synergistic effects of combining the high energy mechanical milling and wet milling on Si negative electrode materials for lithium ion battery. Journal of Power Sources, 2017, 349, 111-120.	7.8	30
48	Rapid crystal growth of bimetallic PdPt nanocrystals with surface atomic Pt cluster decoration provides promising oxygen reduction activity. RSC Advances, 2017, 7, 55110-55120.	3.6	10
49	Amideâ€Functionalized Small Molecules as Solutionâ€Processed Electron Injection Layers in Highly Efficient Polymer Lightâ€Emitting Diodes. Advanced Materials Interfaces, 2016, 3, 1500621.	3.7	5
50	Shell thickness effects on reconfiguration of NiOcore–Ptshell anodic catalysts in a high current density direct methanol fuel cell. RSC Advances, 2016, 6, 72607-72615.	3.6	5
51	Lithiation-induced crystal restructuring of hydrothermally prepared Sn/TiO <sub>2</sub> nanocrystallite with substantially enhanced capacity and cycling performance for lithium-ion battery. RSC Advances, 2016, 6, 48620-48629.	3.6	3
52	Size Effect of Atomic Gold Clusters for Carbon Monoxide Passivation at Rucore–Ptshell Nanocatalysts. Journal of Physical Chemistry C, 2016, 120, 7621-7628.	3.1	3
53	Photolysis and photocatalytic decomposition of sulfamethazine antibiotics in an aqueous solution with TiO <sub>2</sub> . RSC Advances, 2016, 6, 69301-69310.	3.6	48
54	Accumulation of heavy metals and trace elements in fluvial sediments received effluents from traditional and semiconductor industries. Scientific Reports, 2016, 6, 34250.	3.3	74

#	Article	IF	CITATIONS
55	Local heterojunctions of atomic Pt clusters boost the oxygen reduction activity of Rucore@Pdshell nanocrystallites. Journal of Materials Chemistry A, 2016, 4, 17848-17856.	10.3	3
56	Stabilization of Natural Organic Matter by Short-Range-Order Iron Hydroxides. Environmental Science & Technology, 2016, 50, 12612-12620.	10.0	75
57	The size effect of silver nanocubes on gap-mode surface enhanced Raman scattering substrate. Journal of the Taiwan Institute of Chemical Engineers, 2016, 69, 146-150.	5.3	10
58	Molecular Structures of Al/Si and Fe/Si Coprecipitates and the Implication for Selenite Removal. Scientific Reports, 2016, 6, 24716.	3.3	9
59	Self-aligned synthesis of a NiPt-alloycore@Ptshellnanocrystal with contrivable heterojunction structure and oxygen reduction activity. CrystEngComm, 2016, 18, 5860-5868.	2.6	8
60	DNA adsorption by nanocrystalline allophane spherules and nanoaggregates, and implications for carbon sequestration in Andisols. Applied Clay Science, 2016, 120, 40-50.	5.2	37
61	Real-time XRD and XAS investigation on the influences of vanadium additives to the structural chemical state evolutions of LiFePO4of a lithium-ion. Acta Crystallographica Section A: Foundations and Advances, 2015, 71, s343-s343.	0.1	0
62	Mechanism of Arsenic Adsorption on Magnetite Nanoparticles from Water: Thermodynamic and Spectroscopic Studies. Environmental Science & Technology, 2015, 49, 7726-7734.	10.0	314
63	The performance and stability of the oxygen reduction reaction on Pt–M (M = Pd, Ag and Au) nanorods: an experimental and computational study. Chemical Communications, 2015, 51, 6605-6608.	4.1	44
64	The structure-dependent quantum yield of ZnCdS nanocrystals. CrystEngComm, 2015, 17, 5032-5037.	2.6	7
65	Gold atomic clusters extracting the valence electrons to shield the carbon monoxide passivation on near-monolayer core–shell nanocatalysts in methanol oxidation reactions. Physical Chemistry Chemical Physics, 2015, 17, 15131-15139.	2.8	10
66	3D Atomic Arrangement at Functional Interfaces Inside Nanoparticles by Resonant High-Energy X-ray Diffraction. ACS Applied Materials & Interfaces, 2015, 7, 23265-23277.	8.0	10
67	Improving interfacial electron transfer and light harvesting in dye-sensitized solar cells by using Ag nanowire/TiO <sub>2</sub> nanoparticle composite films. RSC Advances, 2015, 5, 70172-70177.	3.6	26
68	Core–shell nanocrystallite growth via heterogeneous interface manipulation. CrystEngComm, 2015, 17, 8623-8631.	2.6	4
69	Local structure distortion induced by Ti dopants boosting the pseudocapacitance of RuO <sub>2</sub> -based supercapacitors. Nanoscale, 2015, 7, 15450-15461.	5.6	22
70	Heterojunction confinement on the atomic structure evolution of near monolayer core–shell nanocatalysts in redox reactions of a direct methanol fuel cell. Journal of Materials Chemistry A, 2015, 3, 1518-1529.	10.3	34
71	Mesoporous TiO2 film modified with a sol–gel based interconnecting network for boosting the dye-sensitized solar cell performance. Thin Solid Films, 2014, 570, 268-272.	1.8	8
72	Structural evolution in LiFePO4-based battery materials: In-situ and ex-situ time-of-flight neutron diffraction study. Journal of Power Sources, 2014, 258, 356-364.	7.8	52

#	Article	IF	CITATIONS
73	Near-Monolayer Platinum Shell on Core–Shell Nanocatalysts for High-Performance Direct Methanol Fuel Cell. Journal of Physical Chemistry C, 2014, 118, 2253-2262.	3.1	28
74	Capacitive performance enhancements of RuO2 nanocrystals through manipulation of preferential orientation growth originated from the synergy of Pluronic F127 trapping and annealing. Nanoscale, 2014, 6, 2861.	5.6	21
75	Graphene-supported Pt and PtPd nanorods with enhanced electrocatalytic performance for the oxygen reduction reaction. Chemical Communications, 2014, 50, 11165-11168.	4.1	39
76	Significance of ions with an ordered arrangement for enhancing the electron injection/extraction in polymer optoelectronic devices. Journal of Materials Chemistry C, 2014, 2, 4805-4811.	5.5	8
77	Oxidation triggered atomic restructures enhancing the electrooxidation activities of carbon supported platinum–ruthenium catalysts. CrystEngComm, 2014, 16, 10066-10079.	2.6	6
78	Correlation between surface state and band edge emission of white light ZnxCd1â^'xS nanocrystals. Journal of Materials Chemistry C, 2014, 2, 2664.	5.5	16
79	Oxidative precipitation of ruthenium oxide for supercapacitors: Enhanced capacitive performances by adding cetyltrimethylammonium bromide. Journal of Power Sources, 2014, 268, 430-438.	7.8	23
80	Real-time investigation on the influences of vanadium additives to theÂstructural and chemical state evolutions of LiFePO 4 for enhancing the electrochemical performance of lithium-ion battery. Journal of Power Sources, 2014, 270, 449-456.	7.8	8
81	Effective anodic oxidation of naproxen by platinum nanoparticles coated FTO glass. Journal of Hazardous Materials, 2014, 277, 110-119.	12.4	35
82	Heterogeneous junction engineering on core–shell nanocatalysts boosts the dye-sensitized solar cell. Nanoscale, 2013, 5, 9181.	5.6	15
83	Thermal-induced growth of RuO <sub>2</sub> nanorods from a binary Ru–Ti oxide composite and alteration in supercapacitive characteristics. Journal of Materials Chemistry A, 2013, 1, 2039-2049.	10.3	20
84	Selenium Speciation in Coal Ash Spilled at the Tennessee Valley Authority Kingston Site. Environmental Science & Technology, 2013, 47, 14001-14009.	10.0	43
85	Core-dependent growth of platinum shell nanocrystals and their electrochemical characteristics for fuel cells. CrystEngComm, 2013, 15, 982-994.	2.6	11
86	Ruthenium core-activated platinum monolayer shell high redox activity cathodic electrocatalysts for dye-sensitized solar cells. Journal of Materials Chemistry A, 2013, 1, 5660.	10.3	12
87	Crystal growth of platinum–ruthenium bimetallic nanocrystallites and their methanol electrooxidation activity. CrystEngComm, 2013, 15, 3932.	2.6	11
88	Enhanced performance of polymer solar cells using solution-processed tetra-n-alkyl ammonium bromides as electron extraction layers. Journal of Materials Chemistry A, 2013, 1, 2582.	10.3	36
89	Formation of self-aggregated and interconnected silver network within sol–gel silica. Journal of Materials Science, 2013, 48, 850-856.	3.7	4
90	Biogeochemical reductive release of soil embedded arsenate around a crater area (Guandu) in northern Taiwan using X-ray absorption near-edge spectroscopy. Journal of Environmental Sciences, 2013, 25, 626-636.	6.1	5

#	Article	IF	CITATIONS
91	The effect of Mn addition on the promotion of oxygen reduction reaction performance for PtCo/C catalysts. Electrochimica Acta, 2013, 105, 180-187.	5.2	15
92	Enhancement of electrochemical properties of Pd/C catalysts toward ethanol oxidation reaction in alkaline solution through Ni and Au alloying. International Journal of Hydrogen Energy, 2013, 38, 4474-4482.	7.1	54
93	Controlling Interconnected Silver Network Structure in Sol–Gel Nanocomposite Via Shrinkageâ€Induced Stress. Advanced Engineering Materials, 2013, 15, 34-39.	3.5	2
94	The structure modification and activity improvement of Pd–Co/C electrocatalysts by the addition of Au for the oxygen reduction reaction. Catalysis Science and Technology, 2012, 2, 1654.	4.1	12
95	Core Dominated Surface Activity of Core–Shell Nanocatalysts on Methanol Electrooxidation. Journal of Physical Chemistry C, 2012, 116, 16969-16978.	3.1	32
96	Structure and magnetism of BaTi1- <i>x</i> Fe <i>x</i> O3- <i>δ</i> multiferroics. Journal of Applied Physics, 2012, 111, .	2.5	6
97	Self-assembled tetraoctylammonium bromide as an electron-injection layer for cathode-independent high-efficiency polymer light-emitting diodes. Journal of Materials Chemistry, 2011, 21, 8715.	6.7	29
98	Tetragonal and hexagonal polymorphs of BaTi1â^'‹i>x‹/i>Fe‹i>x‹/i>O3â^'‹i>Î′‹/i> multiferroics using x-ray and Raman analyses. Applied Physics Letters, 2011, 99, .	3.3	41
99	Hydrogen Spillover Effect of Pt-Doped Activated Carbon Studied by Inelastic Neutron Scattering. Journal of Physical Chemistry Letters, 2011, 2, 2322-2325.	4.6	51
100	Effects of Pt Shell Thicknesses on the Atomic Structure of Ru–Pt Core–Shell Nanoparticles for Methanol Electrooxidation Applications. ChemPhysChem, 2010, 11, 2383-2392.	2.1	58
101	Mechanistic study of arsenate adsorption on lithium/aluminum layered double hydroxide. Applied Clay Science, 2010, 48, 485-491.	5.2	28
102	Fabricating Nanocomposite Catalysts through Interfacial Fusion of Metallic Nanoparticles. Materials Research Society Symposia Proceedings, 2009, 1217, 1.	0.1	1
103	Adsorption mechanism of selenate and selenite on the binary oxide systems. Water Research, 2009, 43, 4412-4420.	11.3	122
104	Hybrid Silver Nanowire/Titanium Oxides Nanocomposites as Anode for Dye ensitized Solar Cell Application. Journal of the Chinese Chemical Society, 2009, 56, 1244-1249.	1.4	16
105	Improved Catalytic Performance of Pt Supported on Multiâ€Wall Carbon Nanotubes as Cathode for Direct Methanol Fuel Cell Applications Prepared by Dualâ€Stepped Surface Thiolation Processes. Journal of the Chinese Chemical Society, 2009, 56, 1236-1243.	1.4	11
106	A Mechanism Study on the Synthesis of Cu/Pd Nanoparticles with Citric Complexing Agent. Journal of Physical Chemistry C, 2007, 111, 12873-12876.	3.1	13
107	Fractal aggregates of the Pt nanoparticles synthesized by the polyol process and poly(N-vinyl-2-pyrrolidone) reduction. Journal of Applied Crystallography, 2007, 40, s540-s543.	4.5	36
108	Arsenate Sorption on Lithium/Aluminum Layered Double Hydroxide Intercalated by Chloride and on Gibbsite:Â Sorption Isotherms, Envelopes, and Spectroscopic Studies. Environmental Science & Technology, 2006, 40, 7784-7789.	10.0	63

#	Article	IF	CITATIONS
109	Catalyst Improvement of Utilization for Direct Methanol Fuel Cell Using Silane Coupling Agents. Electrochemical and Solid-State Letters, 2006, 9, A549.	2.2	3